International Conference on Space Optics—ICSO 2018

Chania, Greece

9–12 October 2018

Edited by Zoran Sodnik, Nikos Karafolas, and Bruno Cugny

Interferometric multi-core fiber optic gyroscope under temperature changing environment

Shinji Mitani

Kenichiro Nigo

Satoshi Karasawa

Haruyuki Endo

et al.

International Conference on Space Optics — ICSO 2018, edited by Zoran Sodnik, Nikos Karafolas, Bruno Cugny, Proc. of SPIE Vol. 11180, 1118055 · © 2018 ESA and CNES · CCC code: 0277-786X/18/$18 · doi: 10.1117/12.2536104

Interferometric multi-core fiber optic gyroscope under temperature changing environment

Shinji Mitani*[a], Kenichiro Nigo[a],
Satoshi Karasawa[b], Haruyuki Endo[b], Taketoshi Takahata[b]
[a]Japan Aerospace Exploration Agency (JAXA), 2-1-1 Sengen, Tsukuba, Ibaraki 305-8508, Japan;
[b]Optoquest Co. Ltd., 1335 Haraichi, Ageo, Saitama 362-0021, Japan

ABSTRACT

We have proposed an interferometric fiber optic gyro (I-FOG) with a novel sensing fiber coil consisting of multi-core fiber (MCF) spliced with fan-in/fan-out (FIFO) devices. This sensing coil can improve the sensitivity of I-FOG without escalating the hardship of winding process of fiber to form coils. We have fabricated a seven-core MCF coil with FIFO devices and demonstrated the proper operation of the proposed I-FOG for the first time. The angular random walk performance of 0.002 deg/√h was achieved, thereby confirming that the seven-core waveguide loop works successfully as a Sagnac interferometer as expected. In addition, we evaluated the effect of temperature changes of MCF and FIFO devices that cause fluctuations in the measured rotation rate. We confirmed that this effect shows essentially the same features as Shupe effect (non-reciprocal phase shift error due to changing environmental temperature) which is a well-known feature of conventional I-FOGs.

Keywords: multi-core fiber, fiber optic gyro, FOG, Sagnac interferometer, Shupe effect, thermally induced phase error

1. INTRODUCTION

Interferometric fiber-optic gyroscope (I-FOG) is a rotation-rate sensor that has been used in numerous types of highly precise and autonomous mobile systems in space, marine and other applications for decades. Improving the sensitivity of I-FOG contributes to open a new era of those mobile systems. One solution for such sensitivity improvement is applying long fiber in the sensing coil. However, tactical-grade I-FOGs have a-few-km length of fiber, and the process of winding such a long length of fiber into multiple layers to form a sensing coil demands unique manufacturing procedures and machines. The problem of I-FOG manufacturing is that this winding process make it inevitable to establish elaborate and costly skills.

To solve this problem, we discuss a new approach by using multi-core fibers (MCFs)[7]. In a past study, the possibility of using MCFs in I-FOGs has been briefly discussed[1], but, the practical implementation of the MCF coil has not been shown yet. In this paper, we explain a novel configuration of a fiber coil using an MCF and a pair of fan-in/fan-out (FIFO) devices that has been proposed in the reference [6]. We also mention that an integrated single optical path can be formed by connecting multiple cores' optical paths in serial. By this connection, the effective fiber length can be increased by a factor of the number of cores, which leads to higher sensitivity.

In this paper, we also show the results of hardware implementation: we fabricated the proposed fiber coil by using a 102-m long, seven-core MCF and implemented it into an open-loop I-FOG system. (Hereafter, we call it 'MC-FOG.') The initial experiment results of this MC-FOG indicate that it has a good linearity in the rotation rate range of up to 10 deg/s and that the angular random walk performance is 0.002 deg/√h. It is mandatory to understand the influence of temperature change in the new parts in I-FOG (i.e. MCF and FIFO devices) because I-FOG is typically sensitive to the change of thermal conditions. We show the dependencies of the measured rotation rate on temperature and temperature change rate as a result of applying heat to the MCF coil, the fan-in device and the fan-out device respectively. Those dependencies appear to be fairly simple and easy to be compensated at this initial evaluation stage, which indicates that its dependency on temperature conditions is not a show-stopper for future MC-FOG development.

*mitani.shinji@jaxa.jp; phone +81-50-3362-7284; fax +81-29-868-5969; jaxa.jp

2. CONCEPT OF INTERFEROMETRIC MULTI-CORE FIBER OPTIC GYROSCOPE

2.1 Operating principle of I-FOG and its problems

We first briefly explain the operation principle of a conventional I-FOG in order to clarify the advantage of using MCF.

Figure 1 shows a schematic of the I-FOG. The signal light (from a broadband light source) is divided by directional coupler 1 (DC1), and the two divided beams propagate in the fiber coil in the clockwise (CW) and counterclockwise (CCW) directions. Then both beams are recombined by DC1.

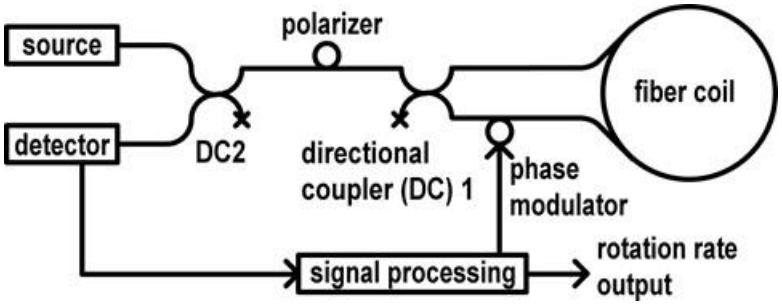

Figure 1. Schematic of conventional I-FOG configuration.

As is well known as the Sagnac effect, a relativistic phase delay occurs depending on the rotation rate, and the phase difference between both beams (in the CW and CCW directions), $\Delta\phi_R$, can be expressed as:

$$\Delta\phi_R = (2\pi LD/\lambda c) \cdot \Omega \quad (1)$$

where Ω is the rotation rate, L is the length of fiber in the coil, D is the diameter of the fiber coil, and λ and c are the wavelength and speed of light in vacuum[2], respectively. Thus, the phase shift is proportional to Ω and can be measured by detecting the interference signal.

In Eq. (1), the scale factor $2\pi LD/\lambda c$ expresses sensitivity relative to the rotation rate, and the design guideline for better sensitivity is to increase L. However, increasing L is not so simple due to a problem intrinsic to the I-FOG, called the Shupe effect[2]. It entails a non-reciprocal phase shift caused by a time-varying distribution of temperature and stress in the fiber coil, and inevitably leads to measurement error depending on the environmental conditions[3]. In order to mitigate the influence of this effect, a unique winding pattern (called symmetrical winding) is typically applied to the coil[4]. This entails, however, a very meticulous winding process, and the number of turns of the fiber coil consequently increases the manufacturing cost.Besides, because an imperfect winding pattern could actually enhance measurement error, it is not easy to make a coil with a long length of fiber.

In short, conventional I-FOGs exhibit practical problems in the manufacturing process when their fiber length is considerably increased for improved sensitivity.

2.2 Proposed fiber coil configuration and its advantages

In order to mitigate the above problems in conventional I-FOGs, we propose a novel sensing fiber coil configuration.

Figure 2 shows a schematic of the proposed fiber coil using an N-core MCF and a pair of FIFO devices. The fiber coil in figure 1 is replaced by this configuration shown in figure 2, and the functions of other I-FOG parts such as the directional couplers, photo detector and light source remains the same.

Here, N-core MCF is just a multicore fiber whose core number is N, and any multicore fiber can be applied to this proposed novel coil configuration: there are no constraints on its core number, core positions and core arrangement in the fiber. FIFO devices have a function for connecting all cores of MCF to those of the corresponding single mode fiber (SMF) as is described as follows.

Port n of the fan-in (FI) device is connected to the port (n-1) of the fan-out (FO) device (n=2,⋯, N). Port 1 of the FI device and port N of the FO device are connected to DC1, and thus serve the role of input/output for the fiber coil. For example, the signal source light is led into emitted from port 1 of the FI device, travels in the CW direction through all the MCF core's waveguides N times, and is derived from port N of the FO device. In this way, an integrated single waveguide loop is realized by using FIFO devices, and the fiber coil's effective optical path length can be increased by a factor of N.

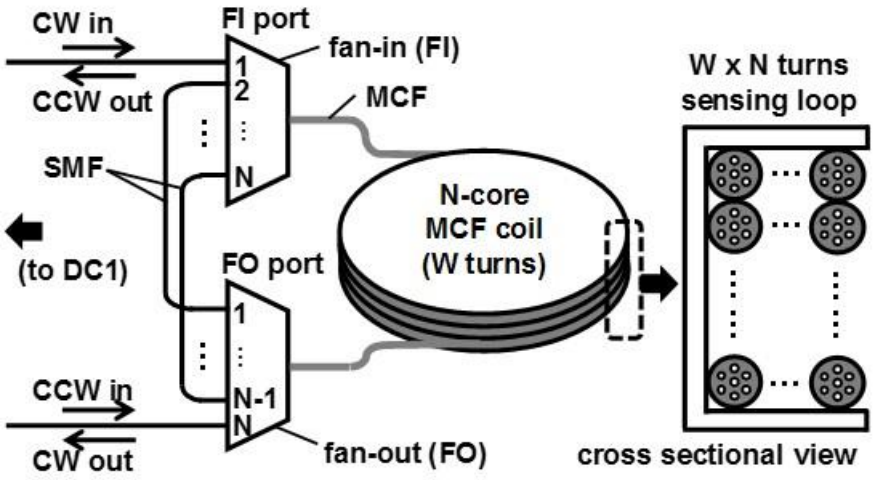

Figure 2. Schematic of the proposed fiber coil using MCF with bundled N-core waveguides.

One of the clear advantages of using MCF is that it allows us to drastically reduce the fiber length while maintaining the gyro's sensitivity. Since the number of turns of the fiber coil becomes $1/N$, the cost of the winding process can also be drastically reduced.

Moreover, due to the small core-pitch of MCF, many core waveguides are densely packed in the coil. This results in the fiber coil being very compact, thereby raising expectations that the influence of the Shupe effect can be suppressed to some extent. Since a time-dependent temperature gradient along the fiber is the cause of the Shupe effect, if different cores experience smaller time-dependent temperature gradient due to the smaller core pitch, then Shupe effect can be also smaller.

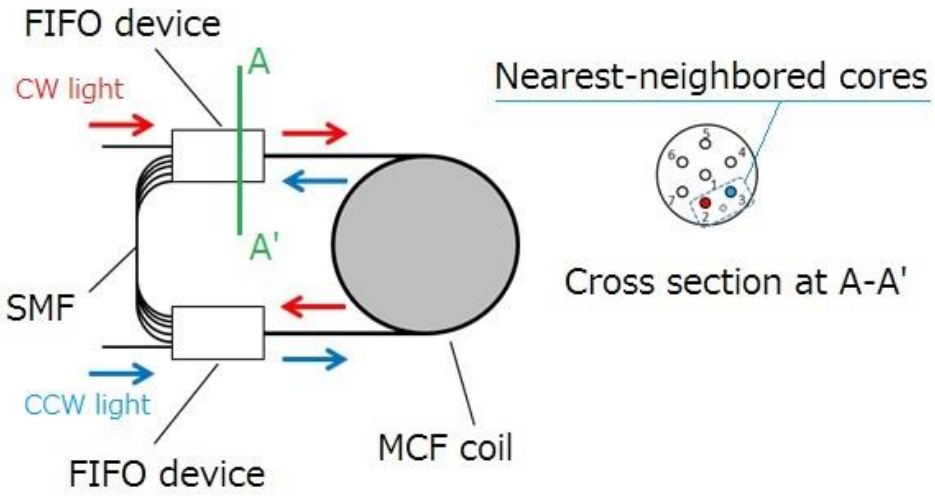

Figure 3. CW light and CCW light are propagating in the nearest-neighbored cores, suppressing the Shupe effect.

Another advantage of using MCF with FIFO devices is the flexibility and comprehensiveness of core-to-core connectivity at the end of MCF. This advantage is particularly effective for MCFs with a large number of cores and/or complex core-arrangement. FIFO devices enable this flexibility in selecting cores to be connected. One of the conceptual examples of making the full use of this flexibility is to select the nearest-neighbored core to guide the light of opposite direction as is shown in Fig. 3. This enables that the CW light and the CCW light experience considerably smaller temperature gradients.

3. EXPERIMENT I: BASIC FUNCTION AND PERFORMANCE

3.1 Fabrication of the proposed sensing fiber coil with MCF and FIFO devices

For demonstration purposes, we fabricated the proposed MCF coil implemented in an I-FOG system. Figure 4 shows a photograph of the fabricated coil. The MCF used in this experiment has a cladding size of 150 μm, and seven cores with a mode field diameter of 10 μm were placed with a core pitch of 45 μm. The fiber loss was 1 dB/km at a wavelength of 1550 nm. A 102.7-m long MCF was wound on a titanium bobbin (Ø128 mm) with the symmetric winding pattern (octupole winding) with a total of eight layers.

Figure 4. Fabricated fiber coil using seven-core MCF and FIFO for demonstration purposes

We also used a pair of FIFO devices based on free-space optics[5], in which each MCF core was coupled to that of a standard SMF. It is worth noting that, compared with other types of FIFOs, these FIFOs have stable low coupling loss, and their core-to-core crosstalk and dependence on polarization are relatively low. These properties are suitable for application in the I-FOG. This FIFO devices and the MCF coil were fusion-spliced. The total optical path length of the fiber coil was 823.8 m. The total insertion loss and polarization-dependent loss of the fiber coil (including the FIFOs) were measured to be 8.4 dB and 0.05 dB, respectively.

3.2 I-FOG configuration with the proposed coil using MCF and FIFO devices

We then constructed an MC-FOG by using the seven-core fiber coil, as shown in Fig. 5. In order to focus on fiber coil performance, we implemented an open-loop system (rather than a digital closed-loop system, which could conceal the coil's imperfection). As a broadband light source, we used a super-luminescent diode (SLD) with output power of 25 mW and a spectral width of 50 nm. The SLD output was led to an integrated optical circuit (IOC) consisting of a Y-branch waveguide and a push-pull phase modulator (for lock-in detection of the phase shift), divided into CW and CCW light

signals, and phase-modulated with a rectangular signal at frequency f_m. We set $f_m$to 127.6 kHz, which corresponds to the inverse of the propagation time of the fiber coil's optical path length.

The signals were then depolarized by passing through the Lyot fiber depolarizer, and led into the fiber coil shown in Fig. 4. The output signals from the fiber coil were recombined at the IOC, and their interference signal was detected by a photodetector (PD). In this experiment, the power received at the PD was measured to be 20.4 μW, which was sufficient for I-FOG operation. By using the lock-in amplifier, we demodulated the amplitude at f_m and derived phase shift $\Delta\phi_R$ (i.e., the rotation rate).

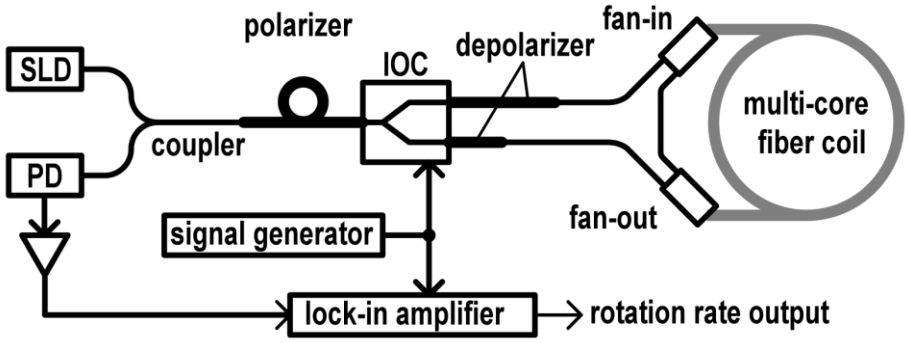

Figure 5. Functional diagram of the implemented MC-FOG open-loop system.

3.3 Results of basic function and performance test

First, we set the fiber coil on the rotation table and measured sensitivity relative to the rotation rate. Figure 6(a) shows the measurement result of the rotation rate in the range of ±10 deg/s (applied around the rate-sensitive axis). As can be seen, the proposed system could sense the rotation rate even at a higher rate of rotation.

Next, in order to evaluate the measurement limit of using this MCF coil, we placed the fiber coil horizontally and recorded the measured rotation rate derived by the proposed system at rest. Figure 6(b) shows the measurement result for 12 hours at a sample rate of 1 Hz. It should be noted that Earth's rotation rate was 8.85 deg/h around the vertical axis at our experiment site (latitude: 36.022°). As can be clearly seen, this system has sufficient performance to sense Earth's rotation rate.

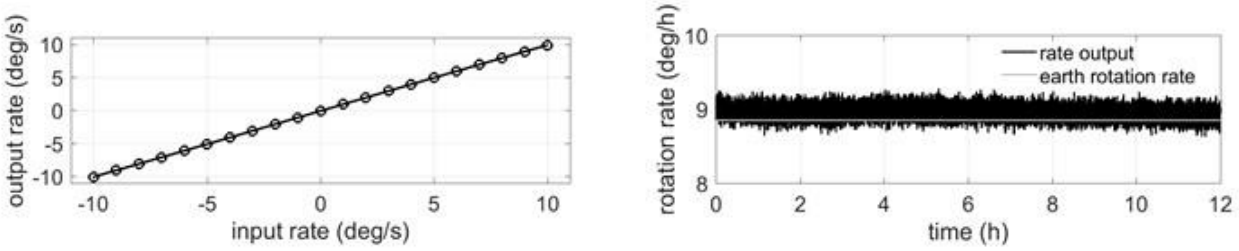

Figure 6. (a) (left) Measured rotation rate in the range of 10 deg/s, (b) (right) Output rate profile of MC-FOG being horizontally and statically placed to measure earth rotation rate (1 Hz sampling)

Figure 7 shows the Allan deviation derived from the data shown in Fig. 6(b). From the part with a $1/\sqrt{\tau}$ slope, we can calculate the angular random walk (ARW). (Note that ARW expresses the power of rate noise in the short term.) From Fig. 7, ARW of this system was measured to be 0.002 deg/√h. We also calculated the theoretical limitation of ARW caused by the shot noise of the signal received at the detector and the excess relative intensity noise (RIN) of the light source[2]. The two solid lines and the dotted line in Fig. 7 show the theoretical ARWs for I-FOGs with 100-m and 700-m long fiber coils,

and measured ARW, respectively. Although only the 102-m long fiber was used, its performance was very close to the theoretical limit of that of the 700-m long fiber coil. In this way, the advantage of using MCF was clearly confirmed.

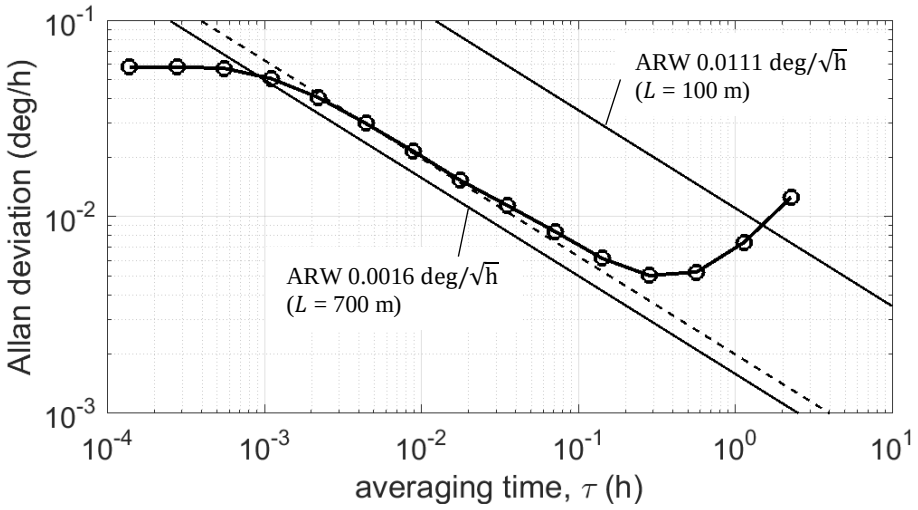

Figure 7. Allan deviation plot and theoretical ARW noise limit

4. EXPERIMENT II: DEPENDENCY ON TEMPERATURE CONDITIONS

4.1 Test settings for heating and temperature measurement

In the proposed MC-FOG, MCF and FIFO devices form some portions of the sensing coil, which means that temperature changes in MCF and FIFO devices are estimated to cause thermally induced fluctuations, that is the Shupe effect. We need to confirm that this estimation is correct and that MCF and FIFO devices do not cause any other major thermally induced effect than Shupe effect; otherwise, the concept of using this novel sensing coil remains unrealistic.

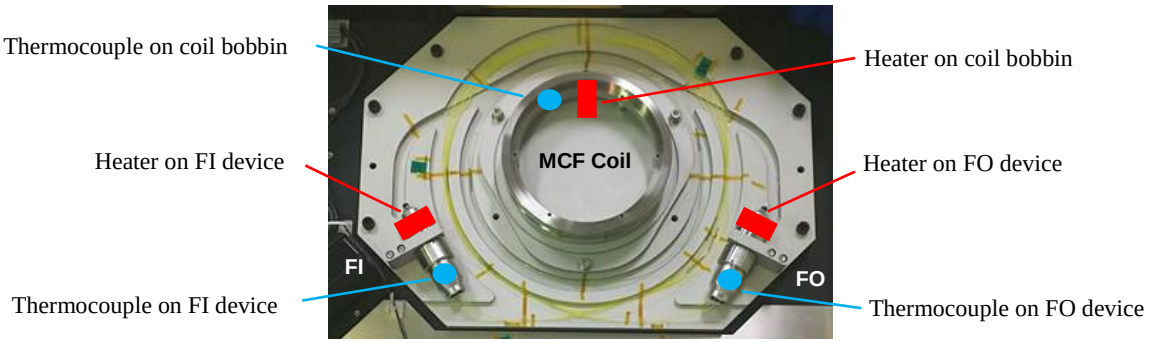

Figure 8. Positions of heaters and thermocouples

For this need, we installed ceramic heaters and thermocouples onto the inner side of the MCF coil bobbin, surfaces of the FI device and FO device. Figure 8 indicates the actual positions of these heaters and thermocouples. All of the proposed MC-FOG system except the signal generator and the lock-in amplifier shown in Fig. 5 was kept in a chamber to avoid any disturbance of air flow. We measured the ambient temperature in the chamber as well.

4.2 Results of dependency on temperature conditions

By heating and natural heat dissipation, we changed the temperature of the MCF coil, the fan-in device and the fan-out device, and evaluated the dependency on the change of temperature conditions of each part in turn.

4.2.1 Dependency on the temperature conditions of MCF coil

The dependency on the temperature change of the MCF coil is shown in Fig. 9. The temperature of the MCF coil is the red-colored line denoted as “coil” in the temperature chart. The change rate of the MCF coil temperature is also shown by the red line denoted as “coil” in the temperature change rate chart. The blue line in the chart of output rate is the measured rotation rate.

At the moment of heater turned on and off, sharp rise and drop in temperature were observed, resulting in the temperature change rate of about ±100 ˚C/h. The temperature change rate dependency is shown on the right side of Fig. 9 clearly exhibits the same linear features as that of conventional I-FOGs. This indicates that simple and precise temperature compensation is possible, which is exemplified by the red line in the chart of output rate. This is the corrected output rate using the coefficient of temperature dependency and temperature change rate dependency shown in Fig. 9.

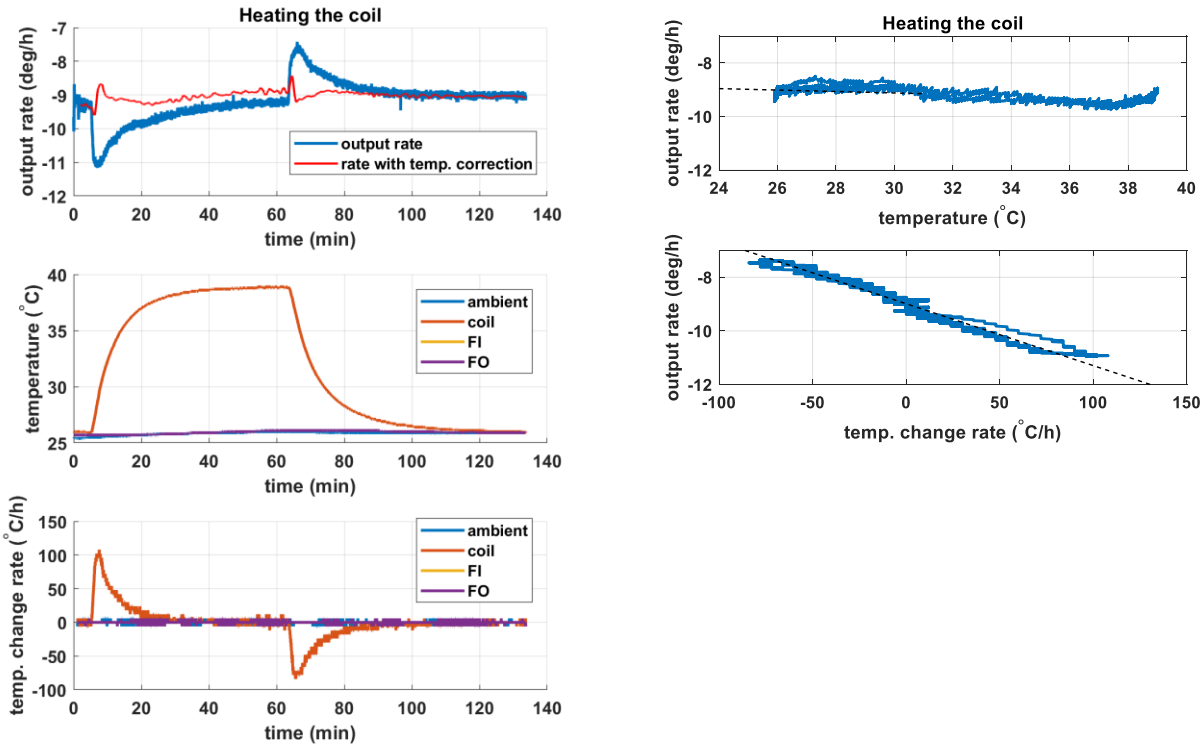

Figure 9. MCF coil’s temperature and its change rate vs. rotation rate (left) and its temperature and temperature change rate dependencies (right)

4.2.2 Dependency on the temperature conditions of FI device and FO device

The dependency on the temperature change of the FI device and the FO device are shown in the left half and the right half of Fig. 10, respectively. The temperature of the FI device and the FO device are the yellow line denoted as “FI” and the purple line denoted as “FO” respectively in their temperature chart. Numerical differentiations of their temperature are also shown in the same manner as their temperature. The blue line in the chart of output rate is the measured rotation rate for both cases of FI device and FO device.

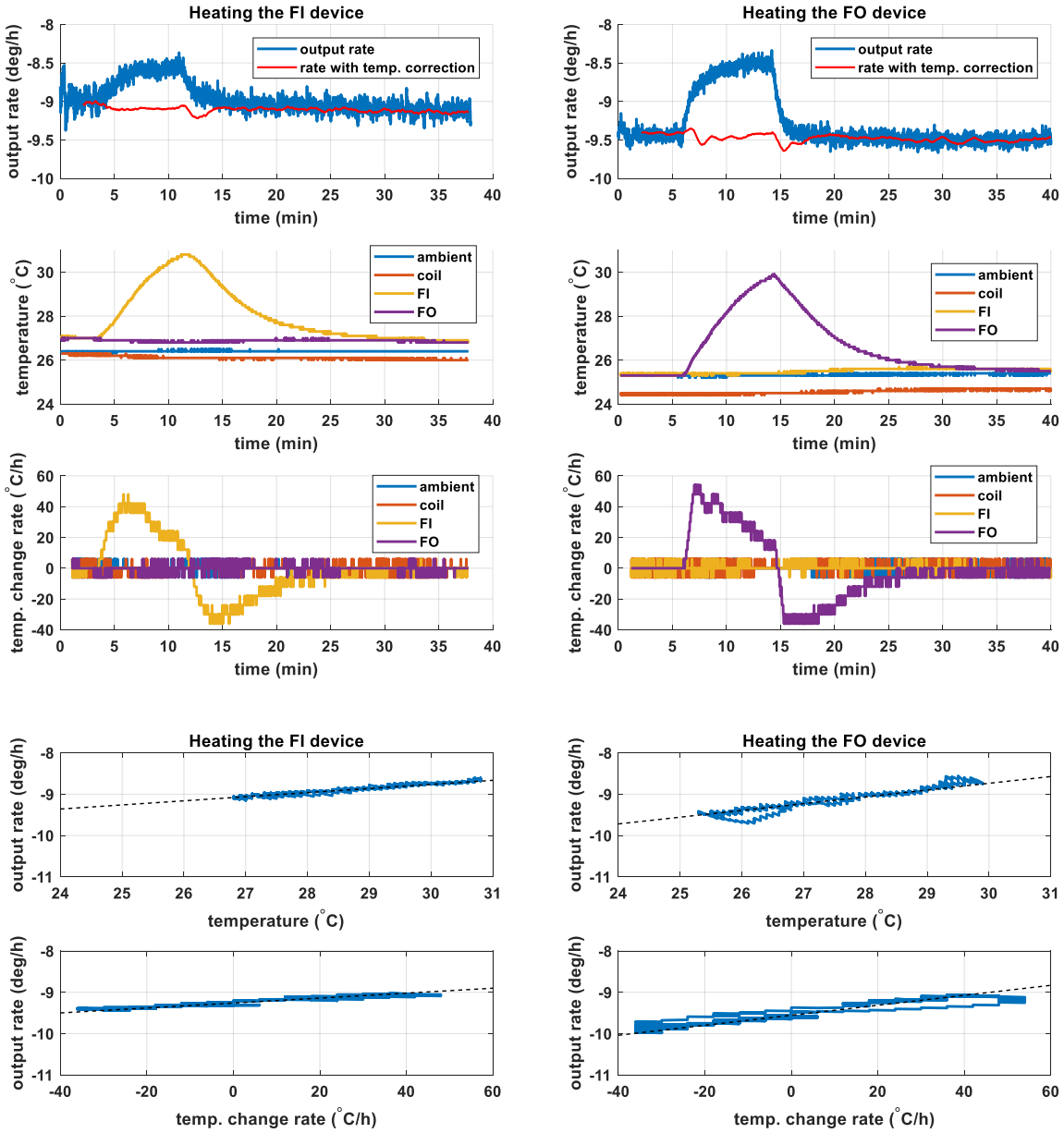

Figure 10. FI device's temperature and its change rate vs. rotation rate (top left) and its temperature and temperature change rate dependencies (bottom left). FO device's temperature and its change rate vs. rotation rate (top right) and its temperature and temperature change rate dependencies (bottom right)

The similar temperature change was observed, although the time for keeping the heater turned on was too short to observe the temperature saturation. The resultant temperature change rates are below ±50 °C/h. However, the temperature change rate dependency shown in Fig. 10 exhibits the same linear features as that of conventional I-FOGs as well as the case of MCF coil. It is also understandable that the dependencies on temperature conditions of FI device and FO device are almost the same since they are symmetrically located in the sensing coil. The red lines in the chart of output rate are an example of corrected output rate using the coefficients of temperature dependency and temperature change rate dependency shown in Fig. 10.

The measured dependencies on temperature conditions are summarized in the Tab. 1. These dependencies appear to be fairly simple and easy to be compensated at this initial evaluation stage. However, we need to consider more factors such as the temperature dependency of the light source and scrutinize those coefficients related to thermal dependency since the fabricated MC-FOG is an open loop I-FOG

Table 1. Summary of the measured dependencies on temperature conditions.

Location of heat load	Temperature dependency [(deg/h)/°C]	Temperature change rate dependency [(deg/h)/(°C/h)]	Figure of plot
MCF Coil	-0.027	-0.023	Fig. 9
FI device	0.099	0.0060	Fig. 10 Left
FO device	0.16	0.012	Fig. 10 Right

5. CONCLUSIONS

We proposed the novel interferometric fiber optic gyro (I-FOG) sensor coil consisting of multi-core fiber (MCF) spliced with fan-in/fan-out (FIFO) devices. We fabricated the seven-core MCF coil with FIFO devices and demonstrated the operation of the proposed I-FOG for the first time. The angular random walk performance of 0.002 deg/$\sqrt{}$h was achieved, thereby confirming that the seven-core waveguide loop works successfully as a Sagnac interferometer as expected. Its dependency on temperature conditions was also measured as an initial evaluation. The dependencies on temperature conditions appear to be fairly simple and easy to be compensated at this initial evaluation stage. Thus, it can be anticipated that its dependency on temperature conditions is not a show-stopper for future MC-FOG development.

ACKNOWLEDGEMENTS

The authors are grateful to S. Nakamura, Y. Takushima (Optoquest Co. Ltd.), and T. Araki (JAXA) for lending their expertise on fiber optic gyroscope and laser optics through useful discussions.

REFERENCES

[1] Bergh, R. A. et al., “Fiber Optic gyro development at Fibernetics,” Proc. of SPIE, Vol. 9852, 98520E (2016).
[2] Lefevre, H. C., “The Fiber-optic Gyroscope Second Edition,” Artech House (2014).
[3] Shupe, D., “Thermally Induced Nonreciprocity in the Fiber-Optic Interferometer,” Applied Optics, Vol. 19, No. 5, p. 654 (1980).
[4] Frigo, N., “Compensation of Linear Sources of Non-reciprocity in Sagnac Interferometers,” Proc. of SPIE, Vol. 412, p. 268 (1983).
[5] Tottori, Y. et al., “Low Loss Optical Connection Module for Seven-Core Multicore Fiber and Seven Single-Mode Fibers,” IEEE Photon. Technol. Lett., Vol. 24, No. 21, p. 1926 (2012).
[6] Mitani, S. et al., “Interferometric Fiber-Optic Gyroscope Using Multi-Core Fiber,” to be presented at 44th European Conference on Optical Communication (2018).
[7] Saito , K., “Multicore Fiber Technology,” Lightwave Technology, Vol.34, No.1 (2016)